JCB Report

Analysis of retrograde transport in motor neurons reveals common endocytic carriers for tetanus toxin and neurotrophin receptor p75^{NTR}

Giovanna Lalli and Giampietro Schiavo

Molecular NeuroPathoBiology Laboratory, Imperial Cancer Research Fund, London WC2A 3PX, United Kingdom

Axonal retrograde transport is essential for neuronal growth and survival. However, the nature and dynamics of the membrane compartments involved in this process are poorly characterized. To shed light on this pathway, we established an experimental system for the visualization and the quantitative study of retrograde transport in living motor neurons based on a fluorescent fragment of tetanus toxin (TeNT H_C). Morphological and kinetic analysis of TeNT H_C retrograde carriers reveals two major groups of organelles: round vesicles and fast tubular structures. TeNT H_C carriers lack markers of the classical endocytic pathway and are not acidified during axonal transport. Importantly, TeNT H_C and NGF share the same retrograde transport organelles, which are characterized by the presence of the neurotrophin receptor p75^{NTR}. Our results provide the first direct visualization of retrograde transport in living motor neurons, and reveal a novel retrograde route that could be used both by physiological ligands (i.e., neurotrophins) and TeNT to enter the central nervous system.

Introduction

Neurons are highly polarized cells characterized by a complex network of trafficking pathways, allowing communication over long distances. Anterograde transport ensures delivery of newly synthesized proteins and organelles to their peripheral destinations (Nakata et al., 1998; Goldstein and Yang, 2000; Kaether et al., 2000). Several organelles and ligands are targeted to the cell body via retrograde transport, which is essential for their biological functions (Goldstein and Yang, 2000). Examples include endogenous molecules, like neurotrophins (Goldstein and Yang, 2000), and pathogens, such as Herpes simplex virus (Bearer et al., 2000).

Recently, much effort has been dedicated to the study of anterograde transport in different types of neurons (Morris and Hollenbeck, 1995; Nakata et al., 1998; Kaether et al., 2000). Retrograde routes were also identified in hippocampal and sympathetic neurons (Parton et al., 1992; Hollenbeck, 1993; Prekeris et al., 1999) by following recycling endosomal markers and fluid phase tracers. However, little is known about the dynamics and the principles regulating retrograde transport.

In this study we sought to investigate this process in living mammalian motor neurons (MNs)* using a nontoxic fragment of tetanus toxin (TeNT). TeNT and its binding fragment provide excellent probes for this purpose because they are among the best examples of ligands undergoing specific uptake and retrograde transport in neurons. TeNT belongs to the clostridial neurotoxin family and enters the nervous system at the neuromuscular junction (NMJ), where it is internalized and retrogradely transported along the MN axons by an unknown mechanism (Schiavo et al., 2000). After reaching the cell body, TeNT is transcytosed into adjacent inhibitory interneurons where it blocks neurotransmitter release, leading to spastic paralysis.

TeNT is composed of a heavy (H) and a light (L) chain linked by a disulphide bond. The L chain is responsible for intracellular activity, whereas the H chain mediates binding and internalization into neurons (Schiavo et al., 2000). The COOH-terminal 50-kD domain of TeNT (H_C) is both necessary and sufficient for binding and internalization in spinal cord cells and purified MNs (Lalli et al., 1999; Herreros et al., 2000). When added to spinal cord cells and to NMJ preparations, TeNT H_C prevents uptake of TeNT, leading

The online version of this article contains supplemental material.

Address correspondence to Giampietro Schiavo, Imperial Cancer Research Fund, 44 Lincoln's Inn Fields, Room 614-5, London WC2A 3PX, UK. Tel.: 44-20-7269-3300. Fax: 44-20-7269-3417. E-mail: g.schiavo@icrf.icnet.uk

Key words: axonal transport; motor neuron; endosome; tetanus toxin; p75^{NTR}

*Abbreviations used in this paper: DIC, differential interference contrast; MN, motor neuron; NMJ, neuromuscular junction; p75^{NTR}, neurotrophin receptor p75; TeNT, tetanus toxin.

to a block of the holotoxin effects and indicating that the H_C binding is fully functional (Lalli et al., 1999). Furthermore, TeNT H_C undergoes axonal retrograde transport in vivo, as shown by the accumulation of H_C in the central nervous system after its intramuscular injection (Schiavo et al., 2000).

In this work we generated a fluorescent TeNT H_C and followed its trafficking in MNs, the cells competent for TeNT endocytosis and transport in vivo. In this cellular system, TeNT H_C is specifically recruited to a novel retrograde transport route, which uses carriers with distinct morphology and average speed. A large fraction of TeNT H_C retrograde organelles is shared by NGF and contains the neurotrophin receptor p75 ($p75^{NTR}$), suggesting that TeNT may use a physiological retrograde transport pathway to reach the soma of MNs.

Results and discussion

Fluorescent TeNT H_C can be used to monitor retrograde transport in living MNs

To create a tool to investigate retrograde transport, we expressed a recombinant TeNT H_C tagged at the NH_2 terminus with a domain containing four cysteines (Griffin et al., 1998), which constitutes a site for preferential modification by thiol-specific fluorescent reagents, such as Alexa Fluor 488 maleimide. The fluorescent TeNT H_C Alexa488 specifically binds, and is internalized by, purified MNs in culture, a process that is prevented by preincubation with an excess of native TeNT (unpublished data).

We used TeNT H_C Alexa488 to follow retrograde transport in living MNs. Cells were incubated with 25–40 nM fluorescent TeNT H_C for 15 min at 37°C, washed, and imaged by confocal or low-light microscopy. The plasma membrane appeared highly stained, particularly at neurite contacts and synaptic sites. Cell bodies and dendrites also displayed a bright staining pattern (Fig. 1 a), suggesting that TeNT H_C binding sites are not restricted to the axonal surface in cultured MNs. An earlier study suggested that TeNT could enter hippocampal neurons through synaptic vesicle recycling (Matteoli et al., 1996). In contrast, in MNs, TeNT H_C is internalized in the absence of depolarization and displays very limited colocalization with synaptic vesicle markers (unpublished data). This is in agreement with reports showing that TeNT uptake and retrograde transport are unaffected at NMJs in which neurotransmitter release has been inhibited (Schiavo et al., 2000). Therefore, the uptake mechanism of TeNT at the NMJ could be different from that occurring in central neurons.

Fluorescent carriers appeared in axons ~20 min after washing the cells. This lag may be due to a maturation phase of the endocytic compartment preceding the loading on transport tracks (Ure and Campenot, 1997). Remarkably, the vast majority of TeNT H_C–labeled structures moved in a retrograde fashion, whereas anterograde vesicles were extremely rare. Low-light time-lapse microscopy revealed the presence of pleiomorphic TeNT H_C carriers (Fig. 1, b–g; Video 1, available at http://www.jcb.org/cgi/content/full/200106142/DC1). We observed slow round vesicles and fast tubules, which continued to move until they disappeared from the field of view. A small fraction of the vesicles were stationary or oscillating, and appeared as bright round structures scattered along axons. We also observed long tubules bending while moving, indicating that they may switch transport tracks en route (Fig. 1, h–j).

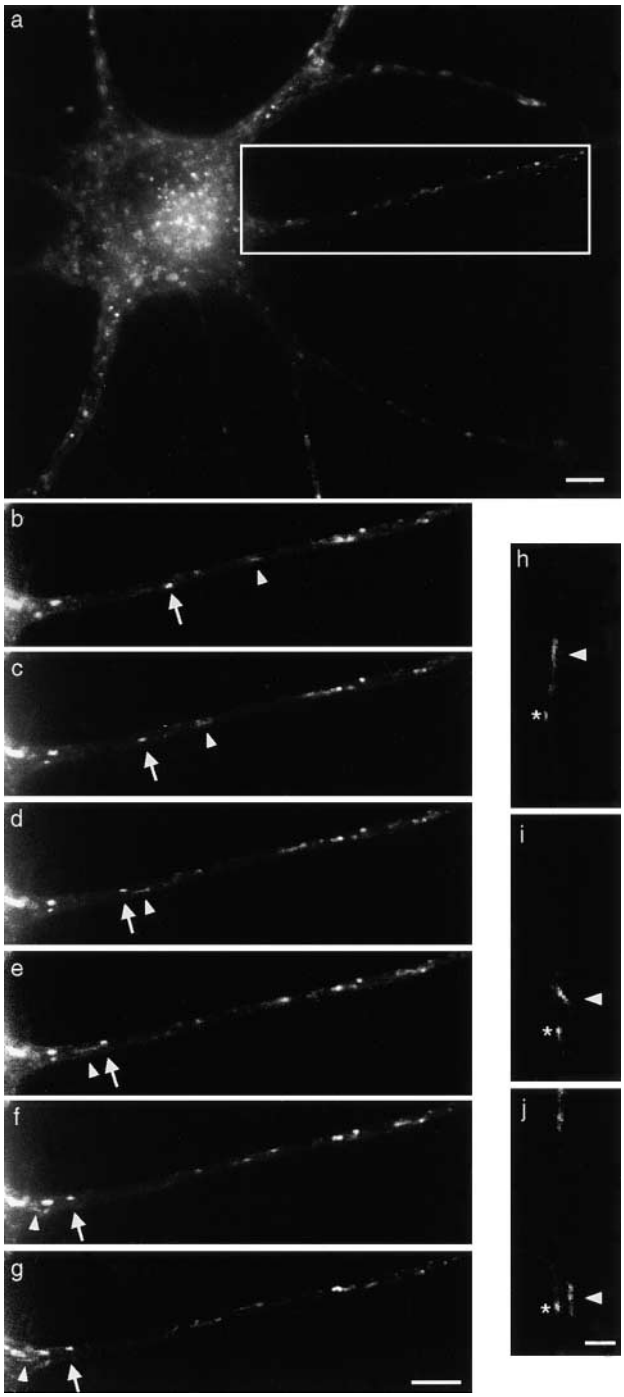

Figure 1. **Visualization of TeNT H_C retrograde carriers.** Cells were incubated with TeNT H_C-Alexa488 for 15 min at 37°C, washed, and imaged by low-light time-lapse microscopy. (a) Low-magnification image of an MN displaying vesicular staining. (b–g) Time series imaging of the axon in the boxed area in a. Intervals between frames are 5 s. Both round vesicles (arrow) and tubular structures (arrowhead) travel toward the cell body (see Video 1, available at http://www.jcb.org/cgi/content/full/200106142/DC1). (h–j) Example of a tubular endosome bending during retrograde transport along a single axon (arrowhead). A slower round vesicle is also indicated (asterisk). The cell body is located out of view at the bottom of the picture. Bars: (a–g) 5 μm; (h–j) 2 μm.

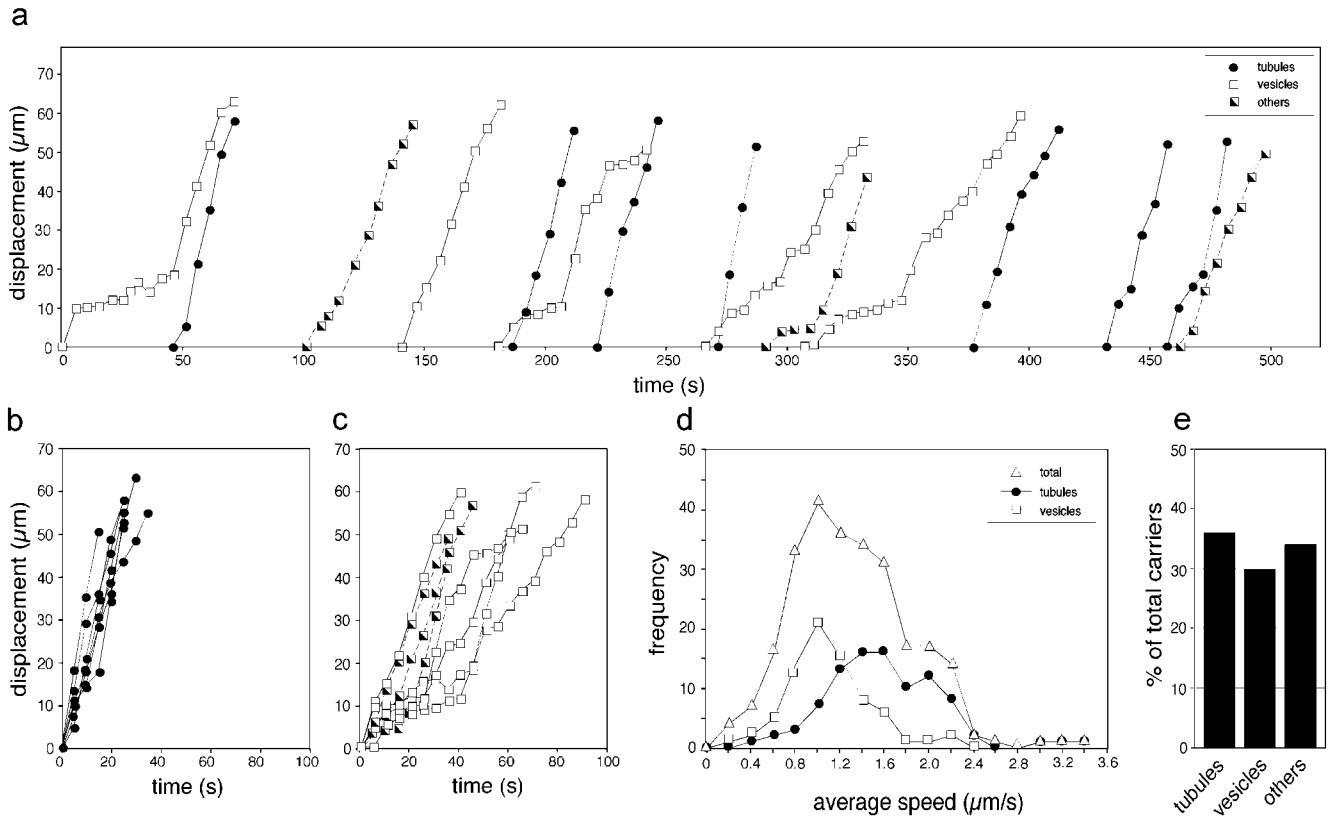

Figure 2. **Kinetic analysis of TeNT H_C carriers in MNs.** (a) Displacement of 15 carriers tracked during a representative experiment. Retrograde movement is conventionally shown as positive. Intervals between time points are 5 s. Note the presence of fast tubules (●) and slower vesicles (□). Half-filled squares refer to other types of carriers. (b) Displacement graphs of the tubules from a, setting the start of tracking as time 0, show an apparently constant movement with similar speed. (c) Displacement graphs of the remaining carriers from a show a slower and more discontinuous movement. (d) Average speeds of TeNT H_C retrograde carriers (△; $n = 256$ carriers from three independent experiments). Round vesicles (□; $n = 76$) have an average speed distribution different from tubules (●, $n = 93$). (e) Percentage of the different types of carriers analyzed in d.

Tracking of TeNT H_C carriers reveals different components of retrograde transport

The kinetics of retrograde transport in living MNs can be analyzed by following the displacement of the TeNT H_C–labeled carriers. Different groups of structures undergoing retrograde transport can be distinguished: tubules (Fig. 2, a and b, ●), which showed a fast movement, and bright round vesicles (Fig. 2, a and c, □) with a slower speed and frequent stationary periods. Other types were rare bright oval bodies and faint round carriers (Fig. 2, a and c, ◩), which displayed all types of movement seen for tubules and bright vesicles. Tubules and vesicles represent the majority of TeNT H_C–labeled structures (66%) (Fig. 2 e).

The average speed distribution of all the retrograde organelles revealed the presence of multiple components (Fig. 2 d, △). Deconvolution analysis confirmed three populations of carriers identified by Gaussian distributions with average speeds of 1.0, 1.5, and 2.1 μm/s, respectively. This trimodal representation allowed the best fitting of the observed average speed curve with lower deviation ($R^2 = 0.996$) than the corresponding bi- or unimodal. Strikingly, this trimodal distribution reflected the speed of the round vesicles, which show a single peak at 1.0 ± 0.29 μm/s (Fig. 2 d, □), and of the faster tubules peaking at 1.5 ± 0.36 and 2.1 ± 0.13 μm/s (Fig. 2 d, ●). Other types of carriers displayed a trimodal distribution as the total frequency curve (unpublished data). In contrast, the rare carriers moving transiently in the anterograde direction presented an average speed of 0.23 μm/s.

These results demonstrate that TeNT H_C uses pleiomorphic axonal carriers, which can be divided in two major morphological classes with distinct kinetic properties: round vesicles and tubulo-vesicular organelles. Retrograde round endosomes had been observed in dorsal root ganglia neurons (Nakata et al., 1998). Long tubules are used for the anterograde delivery of newly synthesized proteins to the neuronal periphery (Nakata et al., 1998; Kaether et al., 2000), whereas bidirectional tubulo-vesicular structures belong to a sorting/recycling compartment in hippocampal neurons (Prekeris et al., 1999). Our study identifies tubular structures as novel axonal carriers characterized by a fast and apparently continuous retrograde movement. The speeds observed for TeNT H_C transport are in the range reported for fast axonal transport (1–5 μm/s) (Nakata et al., 1998; Goldstein and Yang, 2000; Kaether et al., 2000) and closely match those observed for TeNT in vivo (0.8–3.6 μm/s) (Stöckel et al., 1975). Strikingly, TeNT H_C carriers showed a clear bias for retrograde movement, indicating a specific association with one or more types of retrograde motors.

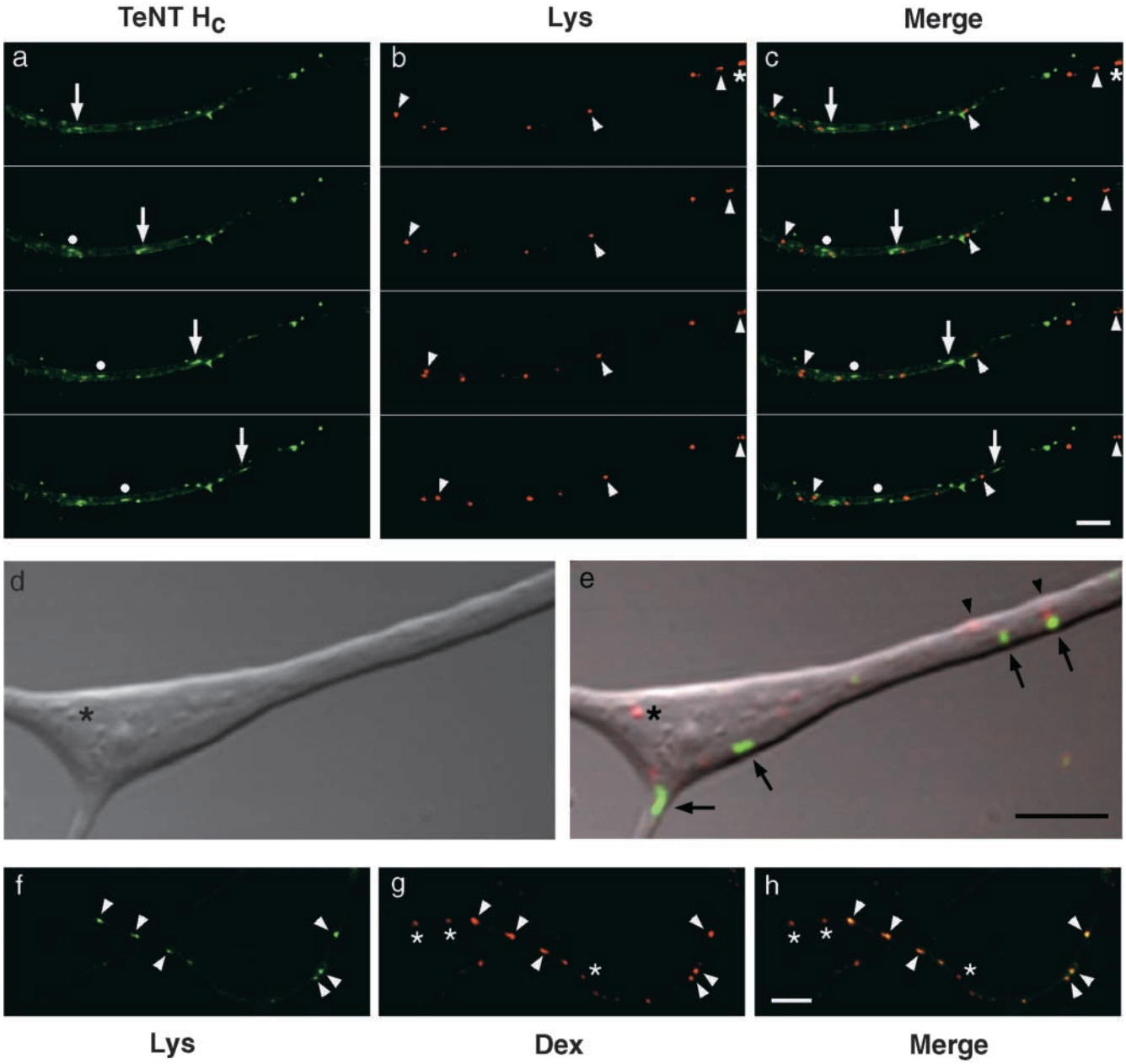

Figure 3. **TeNT H_C carriers do not colocalize with acidic organelles.** MNs were incubated with TeNT H_C Alexa488 and Lysotracker red DND-99 for 20 min at 37°C. Cells were then washed and imaged with low-light microscopy. The cell body is located out of view to the right. Intervals between frames are 5 s. (a) Time series showing retrograde TeNT H_C–labeled endosomes (arrow and ●). (b) Corresponding frames showing Lysotracker-stained organelles (arrowheads). (c) Merged images of a and b. Note the lack of colocalization between TeNT H_C and Lysotracker-stained organelles (see Video 2, available at http://www.jcb.org/cgi/content/full/200106142/DC1). (d–e) Detail from confocal observation of an axonal branch point. (d) DIC image. (e) Overlap of the green and red channels with the simultaneous DIC image. TeNT H_C (green) stains tubular and round carriers (arrows), whereas Lysotracker (red) labels distinct round vesicles (* and arrowheads). An asterisk marks a phase-contrast bright round organelle positive for Lysotracker, but negative for TeNT H_C. (f–h) Lysotracker-positive organelles are accessible to endocytic tracers. MNs were incubated with Texas red dextran overnight and with Lysotracker green DND-26 for 30 min at 37°C. Cells were then washed and imaged by confocal microscopy. Lysotracker-positive organelles (f) are also stained by Texas red dextran (g, arrowheads). (h) Merged image of f and g. Nonacidic organelles containing only dextran are also visible (*). Bars, 5 μm.

TeNT H_C retrograde carriers do not colocalize with acidic organelles and lysosomes

Conflicting results on the fate of TeNT after endocytosis have been reported. Although some suggested that TeNT might escape lysosomal degradation in vivo, others found TeNT in multivesicular bodies and lysosomes (Schiavo et al., 2000). To characterize the TeNT H_C compartment, we performed two-color time-lapse microscopy in living MNs using the membrane-permeable dye Lysotracker, which stains acidic organelles and lysosomes. We observed no colocalization between TeNT H_C–labeled endosomes and Lysotracker-stained vesicles (Fig. 3, a–c; Video 2, available at http://www.jcb.org/cgi/content/full/200106142/DC1). Confocal time-lapse experiments and simultaneous differ-

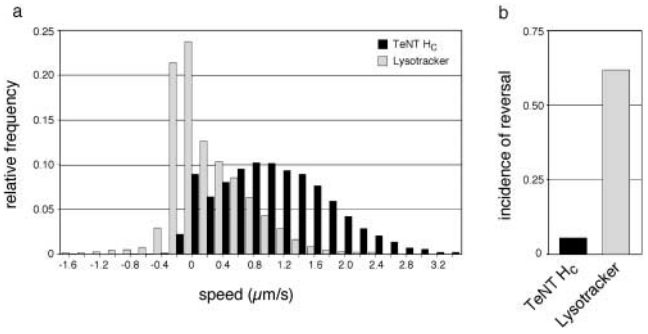

Figure 4. **TeNT H_C carriers and Lysotracker-positive organelles show distinct motile properties.** (a) Relative frequency of speed values observed between two consecutive frames (interval = 5 s) for TeNT H_C carriers (n = 364 vesicles, black bars) and Lysotracker-containing organelles (n = 235 vesicles, gray bars). Retrograde movement is conventionally shown as positive. (b) The incidence of reversal (number of changes of direction per organelle) for Lysotracker-positive vesicles is 11 times higher than TeNT H_C carriers.

ential interference contrast (DIC) imaging revealed that Lysotracker was particularly concentrated in phase-contrast bright round structures (Fig. 3, d–e, *), which are likely to correspond to prelysosomal organelles (Kuznetsov et al., 1992) and were always distinct from the round or tubulovesicular carriers labeled by TeNT H_C and undetectable by DIC (Fig. 3, d–e). The Lysotracker-positive compartment is accessible to the endocytic tracer Texas red dextran (Fig. 3, f–h). Notably, we observed organelles stained by fluorescent dextran, which were not acidic (Fig. 3 h, *).

A comparison of the motile behavior displayed by TeNT H_C– and the Lysotracker-positive organelles further demonstrates that they are distinct compartments (Fig. 4). The speed distribution for TeNT H_C carriers extends to values of >3 μm/s and is retrogradely biased, whereas the organelles stained by Lysotracker are slower and display a higher frequency of anterograde movement (Fig. 4 a). Moreover, Lysotracker vesicles changed direction more frequently compared with TeNT H_C organelles, as shown by the different incidence of reversal (Fig. 4 b). These observations demonstrate that TeNT H_C follows an axonal retrograde route able to bypass lysosomal targeting.

TeNT H_C organelles might be analogous to the Rab11-containing apical recycling compartment described in polarized epithelial (Casanova et al., 1999). Rab11 displayed a ubiquitous punctate staining in MNs. However, very low colocalization with TeNT H_C was observed. TeNT H_C carriers did not contain the early endosome protein EEA1 (Apodaca, 2001), nor the autophagic marker Apg5 and EM analysis excluded the targeting of TeNT H_C to multivesicular bodies (unpublished data). Therefore, TeNT H_C might use a distinct endocytic pathways able to bypass the classical endosomal system, as suggested by the long half-life of TeNT in spinal neurons (Schiavo et al., 2000).

Recently, alternative endocytic routes were shown for Simian Virus 40 (Pelkmans et al., 2001) and *Escherichia coli* (Shin et al., 2000). Both pathogens use intracellular compartments that do not belong to the endosomal–lysosomal system and which involve cholesterol and glycosphingolipid-rich caveolae. Interestingly, cholesterol-enriched rafts have recently been shown to be important for neuronal intoxication by TeNT (Herreros et al., 2001). In MNs, for at least 2 h after internalization, TeNT H_C compartments are not acidic and do not correspond to lysosomes along the entire axonal length nor at branch points. It was previously proposed that a restricted area of the distal axon (50–150 μm from the growth cone) and axonal branch points are major sites of acidification in the progression from endosomes to lysosomes (Overly and Hollenbeck, 1996). Our results strongly suggest that whereas endosomes are acidified by the time they reach the proximal portion of the axon, TeNT H_C carriers are not. This could have important functional consequences, as TeNT has to be protected from acidification and degradation during transport to reach the adjacent interneuron in a fully active form.

TeNT H_C and NGF share retrograde transport carriers

To gain insights into physiological cargoes of this endocytic compartment, we analyzed whether ligands known to undergo retrograde transport in vivo are recruited into TeNT H_C carriers. NGF is retrogradely transported by newborn MNs (Yan et al., 1988) and has transport rates similar to TeNT in sensory and adrenergic neurons (Stöckel et al., 1975). In MNs, NGF-containing retrograde carriers could be detected ~45 min after the end of the incubation at 37°C, consistent with previous studies that used ^{125}I-NGF in sympathetic neurons (Ure and Campenot, 1997). We detected substantial colocalization between TeNT H_C and NGF, with 72% of retrograde organelles being double labeled (n = 106 carriers; two independent experiments). These organelles always corresponded to round vesicles (Fig. 5, a–c; Video 3, available at http://www.jcb.org/cgi/content/full/200106142/DC1). In contrast, we could not observe NGF in retrograde tubules containing TeNT H_C (Fig. 5, e–g), suggesting that tubules and round carriers may belong to different retrograde pathways.

In MNs, retrograde transport of NGF has been suggested to be dependent on $p75^{NTR}$ (Yan et al., 1993, 1988). Strikingly, >80% of TeNT H_C carriers colocalized with $p75^{NTR}$ in axons in absence of exogenous NGF (n = 572 organelles; two independent experiments) (Fig. 5, h–j). Therefore, $p75^{NTR}$ represents the first membrane marker of the retrograde endocytic pathway used by TeNT H_C.

Endogenous ligands like neurotrophins might enter a retrograde transport pathway similar to the one used by TeNT to escape degradation and to reach intact the neuronal cell body. Indeed, NGF injected intramuscularly accumulates in spinal cord MNs without being degraded (Yan et al., 1988). Similar retrograde transport rates for TeNT and NGF have been reported in adrenergic neurons in vivo (Stöckel et al., 1975), which are consistent with the speed observed in our time-lapse experiments. Although the compartment responsible for $p75^{NTR}$ trafficking is still unknown, recent studies highlighted its association with caveolae-like domains (Huang et al., 1999). On this basis, specialized lipid domains involved in the retrograde transport of $p75^{NTR}$ might play an important role in the trafficking of TeNT and other virulence factors through an endocytic route avoiding degradation.

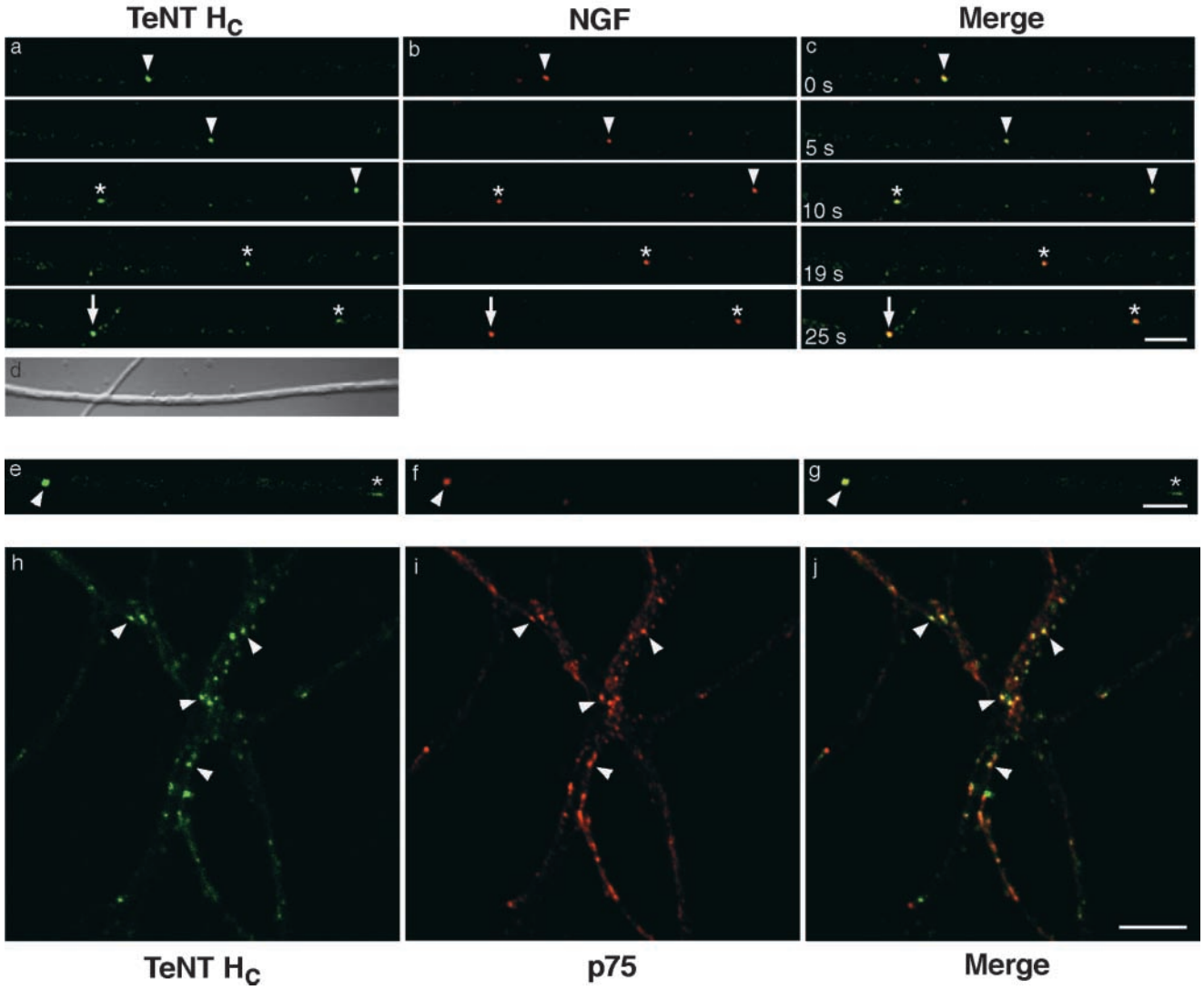

Figure 5. **TeNT H_C retrograde carriers partially colocalize with NGF-labeled compartments.** MNs were incubated with TeNT H_C Alexa488 and Texas red NGF for 30 min at 37°C. Cells were then washed and imaged by time-lapse confocal microscopy. The cell body is located out of view to the right. (a) TeNT H_C Alexa488 and (b) Texas red NGF colocalize in retrograde carriers (arrowhead, asterisk, arrow) (see Video 3, available at http://www.jcb.org/cgi/content/full/200106142/DC1). (c) Merged image of a and b. (d) Corresponding DIC image. TeNT H_C (e) and NGF (f) are found only in round vesicles (arrowhead), whereas tubules appear to be labeled only by TeNT H_C (*). (g) Merged image of e and f. (h–j) Many TeNT H_C carriers colocalize with $p75^{NTR}$ (arrowheads). MNs were incubated with TeNT H_C Alexa488 (h), fixed, immunostained for $p75^{NTR}$ (i), and imaged by confocal microscopy. (j) Merged image of h and i. Bars, 5 μm.

Materials and methods

Materials

Reagents were from Sigma-Aldrich unless otherwise specified. Alexa Fluor 488 maleimide, Texas red sulfonyl chloride, Texas red dextran (mol wt 3,000), Texas red–conjugated goat anti–rabbit secondary antibodies, Lysotracker red DND-99, and Lysotracker green DND-26 were from Molecular Probes. Polyclonal 9992 anti-$p75^{NTR}$ antiserum was a gift from Dr. M. Chao (Skirball Institute, New York University, New York, NY) (Khursigara et al., 1999).

Fluorescent labeling

The preparation of TeNT H_C tagged to the peptide AEAAAREACCRECCAREAAAR will be described elsewhere. Labeling with Alexa Fluor 488 maleimide was performed according to the manufacturer's instructions, and gave an average 1.8 moles of dye per mole of TeNT H_C.

For NGF labeling, 100 μg of mNGF 7S (Alomone Labs) in 500 mM $NaHCO_3$, pH 8.0, was incubated for 1 h at 23°C in the dark with 100 μg of Texas red sulfonyl chloride. Labeled NGF was then purified on a PD-10 column equilibrated with 0.2% acetic acid (Sandow et al., 2000). Texas red NGF contained ~4 moles of dye per mole of protein, and could differentiate PC12 cells similarly to native NGF.

Retrograde transport assay in living MNs

Rat spinal cord MNs were purified from E14 embryos and maintained in culture as described (Herreros et al., 2001). Cells were seeded on glass coverslips or 35-mm glass-bottom microwell dishes (MatTek Corporation) at a density of 40,000 cells/coverslip. After 1 wk in culture, MNs were incubated with 25–40 nM fluorescent TeNT H_C in Neurobasal medium (GIBCO BRL) at 37°C for 15 min, washed three times with DME without phenol red, supplemented with 30 mM Hepes-NaOH, pH 7.3, and then placed in a humidified steel chamber maintained at 37°C. For double-labeling experiments, MNs were incubated with 40 nM TeNT H_C Alexa488 and 50 nM Lysotracker red DND-99 for 20 min at 37°C. For the labeling of endocytic organelles, cells were incubated with 0.9 mg/ml Texas red dextran overnight at 37°C. Lysotracker green DND-26 (80 nM) was then added for 30 min. Cells were washed , and imaged with low-light or confocal microscopy. In another set of experiments, MNs were cooled at 4°C

and incubated with 40 nM TeNT H_C Alexa488 and 40 nM Texas red NGF for 20 min, washed, and then warmed to 37°C. For time-lapse low-light microscopy, images were acquired every 1–5 s with a Nikon Diaphot 200 inverted microscope equipped with a Nikon X100, 1.3 NA Plan Fluor oil-immersion objective using a Nikon FITC B-2A filter and a Hamamatsu C4742–95 Orca1 cooled charge-coupled device camera (Hamamatsu Photonic Systems) controlled by the Kinetic AQM 2000 software (Kinetic Imaging Limited). For two-color video microscopy, a double dichroic filter for simultaneous imaging of fluorescein and Texas red was used (Filter Set XF53; Omega Optical). Exposure times were between 300 and 500 ms. For time-lapse confocal microscopy, images were acquired with continuous scanning using a Zeiss LSM 510 microscope equipped with a Zeiss X63, 1.40 NA DIC Plan-Apochromat oil-immersion objective. A region of interest was simultaneously excited using the 488- and 543-nm lines of a krypton–argon and helium–neon lasers, respectively. Images were collected by averaging twice at a single focal plane and the gain/offset parameters were adjusted to prevent bleed-through between channels.

After the transport assay, MNs were processed for immunoflurescence as described previously (Lalli et al., 1999), limiting permeabilisation with 0.1% Triton X-100 to 15 min before blocking.

Tracking and data quantification

The Motion Analysis software (Kinetic Imaging) was used for vesicle tracking. Only moving vesicles that could be tracked for at least three time points were considered. The distance covered by a carrier between two consecutive frames or between the initial and the final tracking points was used to determine speed and average speed, respectively. Statistical analysis was performed using SigmaPlot 2000 (v 6.0; SPSS Science). Curve fitting was obtained by using KaleidaGraph (v.3.5; Synergy Software) and Origin (v.4.0; Microcal Software). Single frame-images were processed for presentation in Adobe Photoshop®5.5.

Online supplemental material

All videos were acquired as described above, processed using Adobe Premiere®, and saved as Quicktime movies, and are available at http://www.jcb.org/cgi/content/full/200106142/DC1.

Video 1 shows that TeNT H_C is retrogradely transported in vesicles and tubules along an MN axon (Fig. 1 a, boxed area). Cells were incubated with TeNT H_C Alexa488 for 15 min at 37°C, washed, and imaged with low-light time-lapse microscopy. The cell body is located on the left. Frames were taken every 5 s. The video consists of 95 frames played at 5 frames/s. The image is 48 μm × 15 μm.

Video 2 shows that TeNT H_C carriers do not colocalize with lysosomes or acidic organelles. Rat MNs were incubated with TeNT H_C Alexa488 (green) and Lysotracker DND-99 (red) for 20 min at 37°C. Cells were washed and imaged with double-color low-light microscopy. The cell body is located to the right. Frames were taken every 5 s. The video consists of 31 frames played at 5 frames/s. The image is 57 μm × 19 μm. (See Fig. 3, a–c).

Video 3 shows that TeNT H_C carriers colocalize with Texas red NGF–labeled compartments. Rat MNs were incubated with TeNT H_C Alexa488 and Texas red NGF for 30 min at 37°C. Cells were then washed and imaged by confocal microscopy. The cell body is located to the right. Frames were taken every 0.24 s. The video consists of 159 frames played at 10 frames/s. The image is 47 μm × 7 μm. (See Fig. 5, a–c).

We thank the members of the ICRF Light Microscopy Laboratory for valuable help with live imaging and tracking, and G. Charras for the mathematical analysis. We are also grateful to Drs. T. Clandinin, C. Dotti, E. Lalli, C. Montecucco D. Shima, S. Tooze, G. Warren and members of the Molecular NeuroPathoBiology Laboratory for critical reading of the manuscript.

This work was supported by the Imperial Cancer Research Fund.

Submitted: 26 June 2001
Revised: 28 November 2001
Accepted: 30 December 2001

References

Apodaca, G. 2001. Endocytic traffic in polarized epithelial cells: role of the actin and microtubule cytoskeleton. *Traffic.* 2:149–159.

Bearer, E.L., X.O. Breakefield, D. Schuback, T.S. Reese, and J.H. LaVail. 2000. Retrograde axonal transport of herpes simplex virus: evidence for a single mechanism and a role for tegument. *Proc. Natl. Acad. Sci. USA.* 97:8146–8150.

Casanova, J.E., X. Wang, R. Kumar, S.G. Bhartur, J. Navarre, J.E. Woodrum, Y. Altschuler, G.S. Ray, and J.R. Goldenring. 1999. Association of Rab25 and Rab11a with the apical recycling system of polarized Madin-Darby canine kidney cells. *Mol. Biol. Cell.* 10:47–61.

Goldstein, L.S., and Z. Yang. 2000. Microtubule-based transport systems in neurons: the roles of kinesins and dyneins. *Annu. Rev. Neurosci.* 23:39–71.

Griffin, B.A., S.R. Adams, and R.Y. Tsien. 1998. Specific covalent labeling of recombinant protein molecules inside live cells. *Science.* 281:269–272.

Herreros, J., G. Lalli, C. Montecucco, and G. Schiavo. 2000. Tetanus toxin fragment C binds to a protein present in neuronal cell lines and motoneurons. *J. Neurochem.* 74:1941–1950.

Herreros, J., T. Ng, and G. Schiavo. 2001. Lipid rafts act as specialised domains for tetanus toxin binding and internalisation into neurons. *Mol. Biol. Cell.* 12: 2947–2960.

Hollenbeck, P.J. 1993. Products of endocytosis and autophagy are retrieved from axons by regulated retrograde organelle transport. *J. Cell Biol.* 121:305–315.

Huang, C.S., J. Zhou, A.K. Feng, C.C. Lynch, J. Klumperman, S.J. DeArmond, and W.C. Mobley. 1999. Nerve growth factor signaling in caveolae-like domains at the plasma membrane. *J. Biol. Chem.* 274:36707–36714.

Kaether, C., P. Skehel, and C.G. Dotti. 2000. Axonal membrane proteins are transported in distinct carriers: a two-color video microscopy study in cultured hippocampal neurons. *Mol. Biol. Cell.* 11:1213–1224.

Khursigara, G., J.R. Orlinick, and M.V. Chao. 1999. Association of the p75 neurotrophin receptor with TRAF6. *J. Biol. Chem.* 274:2597–2600.

Kuznetsov, S.A., G.M. Langford, and D.G. Weiss. 1992. Actin-dependent organelle movement in squid axoplasm. *Nature.* 356:722–725.

Lalli, G., J. Herreros, S.L. Osborne, C. Montecucco, O. Rossetto, and G. Schiavo. 1999. Functional characterisation of tetanus and botulinum neurotoxins binding domains. *J. Cell Sci.* 112:2715–2724.

Matteoli, M., C. Verderio, O. Rossetto, N. Iezzi, S. Coco, G. Schiavo, and C. Montecucco. 1996. Synaptic vesicle endocytosis mediates the entry of tetanus neurotoxin into hippocampal neurons. *Proc. Natl. Acad. Sci. USA.* 93: 13310–13315.

Morris, R.L., and P.J. Hollenbeck. 1995. Axonal transport of mitochondria along microtubules and F-actin in living vertebrate neurons. *J. Cell Biol.* 131: 1315–1326.

Nakata, T., S. Terada, and N. Hirokawa. 1998. Visualization of the dynamics of synaptic vesicle and plasma membrane proteins in living axons. *J. Cell Biol.* 140:659–674.

Overly, C.C., and P.J. Hollenbeck. 1996. Dynamic organization of endocytic pathways in axons of cultured sympathetic neurons. *J. Neurosci.* 16:6056–6064.

Parton, R.G., K. Simons, and C.G. Dotti. 1992. Axonal and dendritic endocytic pathways in cultured neurons. *J. Cell Biol.* 119:123–137.

Pelkmans, L., J. Kartenbeck, and A. Helenius. 2001. Caveolar endocytosis of simian virus 40 reveals a new two-step vesicular-transport pathway to the ER. *Nat. Cell Biol.* 3:473–483.

Prekeris, R., D.L. Foletti, and R.H. Scheller. 1999. Dynamics of tubulovesicular recycling endosomes in hippocampal neurons. *J. Neurosci.* 19:10324–10337.

Sandow, S.L., K. Heydon, M.W. Weible II, A.J. Reynolds, S.E. Bartlett, and I.A. Hendry. 2000. Signalling organelle for retrograde axonal transport of internalized neurotrophins from the nerve terminal. *Immunol. Cell Biol.* 78:430–435.

Schiavo, G., M. Matteoli, and C. Montecucco. 2000. Neurotoxins affecting neuroexocytosis. *Physiol. Rev.* 80:717–766.

Shin, J.S., Z. Gao, and S.N. Abraham. 2000. Involvement of cellular caveolae in bacterial entry into mast cells. *Science.* 289:785–788.

Stöckel, K., M. Schwab, and H. Thoenen. 1975. Comparison between the retrograde axonal transport of nerve growth factor and tetanus toxin in motor, sensory and adrenergic neurons. *Brain Res.* 99:1–16.

Ure, D.R., and R.B. Campenot. 1997. Retrograde transport and steady-state distribution of ^{125}I-nerve growth factor in rat sympathetic neurons in compartmented cultures. *J. Neurosci.* 17:1282–1290.

Yan, Q., W.D. Snider, J.J. Pinzone, and E.M. Johnson, Jr. 1988. Retrograde transport of nerve growth factor (NGF) in motoneurons of developing rats: assessment of potential neurotrophic effects. *Neuron.* 1:335–343.

Yan, Q., J.L. Elliott, C. Matheson, J. Sun, L. Zhang, X. Mu, K.L. Rex, and W.D. Snider. 1993. Influences of neurotrophins on mammalian motoneurons in vivo. *J. Neurobiol.* 24:1555–1577.